

## GEOTHERMAL FIELDS AND THERMAL PROCESSES IN CRYOSPHERE

## VARIATIONS IN THERMAL DIFFUSIVITY OF THE TUNDRA COVER ACCORDING TO DATA FROM FIELD OBSERVATIONS DURING THE SUMMER PERIOD

S.G. Kornienko

*Oil and Gas Research Institute, Russian Academy of Sciences,  
Gubkina str. 3, Moscow, 119333 Russia; spaceakm2@ogri.ru*

Summer thermometric observations in the area of the Yamburg oil and gas condensate field have been used to calculate thermal diffusivity of moss (*Sphagnum fuscum*), shrubby lichen (*Cladonia arbuscula*), and two-layer samples of soil-vegetation cover consisting of mixed vegetation (*Empetrum nigrum*, *Vaccinium vitis-idaea*, *Carex arctisibirica*) of varying thickness and sandy soil. For sphagnum and lichens, thermal diffusivity has been calculated for the periods with different weather conditions. Thermal diffusivity values obtained during the experiment are quite close to the previously published data on similar types of the tundra cover. At a depth of 12 cm, the amplitude of daily temperature fluctuations under the vegetation cover decreases by 84–94 %. Its decrease by 37 % takes place in the upper layer of the tundra cover of 4.2–6.4 cm in thickness in dependence on the type of the cover. An abnormally high increase in thermal diffusivity of sphagnum moss takes place upon an increase in air humidity and precipitation at the end of summer. This fact confirms the unique thermal insulation properties of sphagnum moss providing conservation of ice wedges in the areas of drained sediments. At the mean daily air temperatures below 27 °C and relative air humidity above 49 %, the thermal diffusivity of the studied samples of the soil-surface cover can serve as an indicator of their thermal insulating properties.

**Keywords:** thermal diffusivity, soil-vegetation cover, tundra, air temperature, water content

## INTRODUCTION

Relevance of in situ studies of the thermophysical properties of tundra vegetation is specified by the need to obtain objective data on the state and possible transformation of permafrost under the existing climatic trends and anthropogenic impacts. Changes in thermal insulation properties of the ground cover in the permafrost zone are one the main factors affecting the depth of seasonal thawing and the volume of greenhouse gas emission. An increase in the mean annual air temperature in the northern latitudes [Vasil'iev *et al.*, 2020] is accompanied by changes in the species composition and density of vegetation cover, which, under certain conditions, may lead to either degradation or aggradation of permafrost [Konishchev, 2009; Anisimov and Sherstyukov, 2016]. Satellite images clearly indicate that modern climate warming has already led to increased productivity of tundra vegetation and greening of the Arctic [Beck and Goetz, 2011; Urban *et al.*, 2014; Bhatt *et al.*, 2017]. Simultaneous changes in climate and phytocenoses in the recent decades demonstrate the large-scale feedbacks in the Arctic and Subarctic ecosystems.

The soil-vegetation cover (SVC) plays a key role in the heat exchange of permafrost with the atmosphere. The SVC is understood as the upper part of the active layer composed of the aboveground vegetation cover, litter, peat, or sod layer, and organic substrate. The influence of the tundra SVC on the tem-

perature regime of soils can be estimated by thermal diffusivity ( $K$ ) calculated from the daily temperature differences on the surface and at the bottom of the SVC [Ershov, 2004]. The thermal diffusivity was chosen as a possible indicator of thermal insulating properties of SVC *in situ* primarily because of the simplicity of measurements with the use of temperature loggers. Temperature loggers are commonly used in geocryological studies; however, there are hardly any results of their application in the study of variations in the thermal diffusivity of the tundra cover. In the context of such studies, data on the relationship between the thermal diffusivity of typical species of the tundra cover and weather conditions, first of all, air humidity, is also essential. The purpose of this work is to study and characterize variations in the thermal diffusivity values for the several types of the tundra SVC in the summer period under natural conditions. These studies included:

- Testing the techniques for determining the SVC thermal diffusivity *in situ* on the basis of the long-term measurements using temperature loggers;
- Characterizing the relationship between the thermal diffusivity of different types of the tundra cover and weather conditions;
- Assessing the use of thermal diffusivity values as indicators of thermal insulating properties of the SVC.

**EXPERIENCE IN STUDYING THERMOPHYSICAL PROPERTIES OF THE TUNDRA SOIL-VEGETATION COVER**

Mosses, lichens, shrubs, and herbs predominate in the SVC of the Arctic and Subarctic tundra [Ershov, 2004; Morozova and Magomedova, 2004]. A thickness of a moss mat varies from 0.01 to 0.2 m; sometimes, it can reach 0.5 m. Thermophysical properties of soils and peat have been well studied. Less is known about thermophysical properties of mosses, lichens, and vascular plants.

Thermal diffusivity ( $K$ ) of the tundra cover can be determined in situ from data on the attenuation of the amplitude of daily temperature fluctuation (DTF) with depth [Ershov, 2004]:

$$K = \frac{\pi z^2}{\tau_{\text{day}} (\ln A_1 - \ln A_2)^2}, \quad (1)$$

where  $A_1$  and  $A_2$  are DTF amplitudes at the surface of the cover and at a depth  $z$ , respectively;  $\tau_{\text{day}}$  is the period of temperature fluctuations (usually, one day).

Table 1. **Thermophysical properties of the samples of the tundra cover in the unfrozen state**

No.	Cover type	$\rho_d$ , g/cm <sup>3</sup>	$W_n$ , %	$\lambda$ , W/(m·K)	$C_n \cdot 10^{-6}$ , W·s/(m <sup>3</sup> ·K)	$K \cdot 10^7$ , m <sup>2</sup> /s	Source
1	17 bryophyte species	0.02–0.08	0–80	0.05–0.50	0.3–4.0	–	[Soudzilovskaia et al., 2013]
2	Green moss	0.18	0–90	0.05–0.29	0.3–4.0	0.7–1.4	[Gavril'ev, 2004]
3	Sod, moss, lichen, herbaceous vegetation	–	8–80	0.05–0.50	–	0.8–1.3	[Aleksyutina and Motenko, 2012]
4	Moss-lichen	–	0–100	0.05–0.48	0.5–3.9	0.9–1.2*	[Porada et al., 2016]
5	Lichen	0.07	18	0.22	–	–	[Mandarov and Skryabin, 1978]
6	Moss brown	0.15	41	0.23	–	–	[Mandarov and Skryabin, 1978]
7	Sphagnum moss	0.18	17	0.28	–	–	[Mandarov and Skryabin, 1978]
8	Lichen	0.06	12	0.15	–	–	[Pavlov, 1980]
9	Moss brown, green and others	0.12	34	0.22	–	–	[Pavlov, 1980]
10	Sphagnum moss	0.12	43	0.28	–	–	[Pavlov, 1980]
11	Moss ( <i>Sanionia uncinata</i> )	0.096	14*	0.17	–	–	[Osokin and Sosnovsky, 2012]
12	Moss ( <i>Hylocomium splendens</i> var. <i>alaskanum</i> )	0.059	12*	0.13	–	–	[Osokin and Sosnovsky, 2012]
13	Lichen	–	–	0.13*	–	–	[Fel'dman et al., 1988]
14	Green moss	–	–	0.16*	–	–	[Fel'dman et al., 1988]
15	Sphagnum	–	–	0.31*	–	–	[Fel'dman et al., 1988]
16	Sod	–	–	0.40*	–	–	[Fel'dman et al., 1988]
17	Sphagnum moss	–	–	0.07–0.19	–	–	[Fukui et al., 2008]
18	Feather mosses ( <i>Hylocomium splendens</i> and <i>Pleurozium schreberi</i> )	0.02–0.12	0–40	0.02–0.2	–	–	[O'Donnell et al., 2009]
19	Sphagnum ( <i>Sphagnum fuscum</i> )	0.04–0.17	0–90	0.03–0.43	–	–	[O'Donnell et al., 2009]
20	Moss ( <i>Tomentypnum nitens</i> )	–	–	–	–	1.1*	[Gornall et al., 2007]
21	Moss-lichen	–	–	–	–	1.8*	[Pavlov, 1979]
22	Sedge-sphagnum	–	–	–	–	2.8*	[Pavlov, 1979]
23	Sphagnum-shrubby	–	–	–	–	1.4*	[Pavlov, 1979]
24	Green moss (with low water content)	–	–	0.19	–	1.0	[Ershov, 2004]
25	Lichen (reindeer lichen, dry)	–	–	0.17	–	–	[Ershov, 2004]

Note:  $\rho_d$  – dry unit weight,  $W_n$  – volumetric water content,  $\lambda$  – thermal conductivity coefficient,  $C_n$  – volumetric heat capacity,  $K$  – thermal diffusivity.

\* Values calculated from the data given in the source.

The real tundra SVC is a multilayer medium with heterogeneous thermophysical properties. In addition, heat exchange in a more porous upper layer of vegetation may have a convective component [Stepanenko et al., 2020]. Therefore, under natural conditions, only effective values of the thermal diffusivity of the SVC can be estimated experimentally. An effective value of thermal diffusivity means the  $K$  value of the heterogeneous (in thickness) SVC equivalent to the  $K$  value of the homogeneous SVC of the same thickness and under the same conditions of nonstationary thermal influence. The thickness of the near-surface layer ( $D$ ), in which the amplitude of daily temperature fluctuations attenuates by 37 %, is determined by the formula [Stoy et al., 2012]:

$$D = \frac{z}{\ln A_1 - \ln A_2}. \quad (2)$$

The parameter characterizing the degree of DTF damping to a depth  $z$  can be calculated by a formula:

$$M = \frac{A_1 - A_2}{A_1} \cdot 100\%. \quad (3)$$

If the thermal conductivity coefficient ( $\lambda$ ) and bulk heat capacity ( $C_n$ ) are known,  $K$  can be calculated from their ratio:

$$K = \lambda / C_n. \quad (4)$$

Table 1 demonstrates the values of dry unit weight ( $\rho_d$ ), volumetric water content ( $W_n$ ), volumetric heat capacity, thermal conductivity, and thermal diffusivity of the SVC samples in the unfrozen state, including those calculated from the data given in sources using Eqs. (1) and (4), as well as the relations between the volumetric and gravimetric water contents of the samples.

Having analyzed 17 moss species [Soudzilovskaia et al., 2013], it was concluded that the thermal insulating properties of mosses do not depend on their density, but only on the water content and the mat thickness. This conclusion is generally confirmed by the results given in [Mandarov and Skryabin, 1978; O'Donnell et al., 2009; Porada et al., 2016] (Table 1). On the basis of these data, the dependence  $\lambda(W_n)$  is approximately the same in spite of a rather large scatter of moss densities. The work [Porada et al., 2016] reports on the results of the modeling of the dependences  $\lambda(W_n)$  and  $C_n(W_n)$  for the bryophyte-lichen mat 4.5 cm thick and porosity of 80 %. The properties of mosses (without specifying the species) growing on the high drained areas have been considered, as well as the properties of lichens, because they are close to feather mosses in terms of density and the mechanism of water saturation [Stoy et al., 2012].

## STUDY OBJECTS

The study area is located in the central part of the Taz Peninsula, in the Poilovoyakha River basin, within the territory of the Yamburg oil and gas condensate field (OGCF). This area belongs to the subzone of southern Subarctic tundras. Figure 1 demonstrates the location of the study area and observation sites as seen on satellite images [https://earth.google.com.my/]. The Zyryanskaya and Kazantsevskaya marine plains and erosion-accumulative surfaces of river floodplains and terraces determine the relief of this area [Pavlinin et al., 2015]. The surfaces unaffected by gully erosion are flat, with insignificant differences in elevation. Observation sites (Fig. 1b) belong to the lacustrine-alluvial plain with absolute heights from 26 to 43 m a.s.l. Interfluves are characterized by heavy

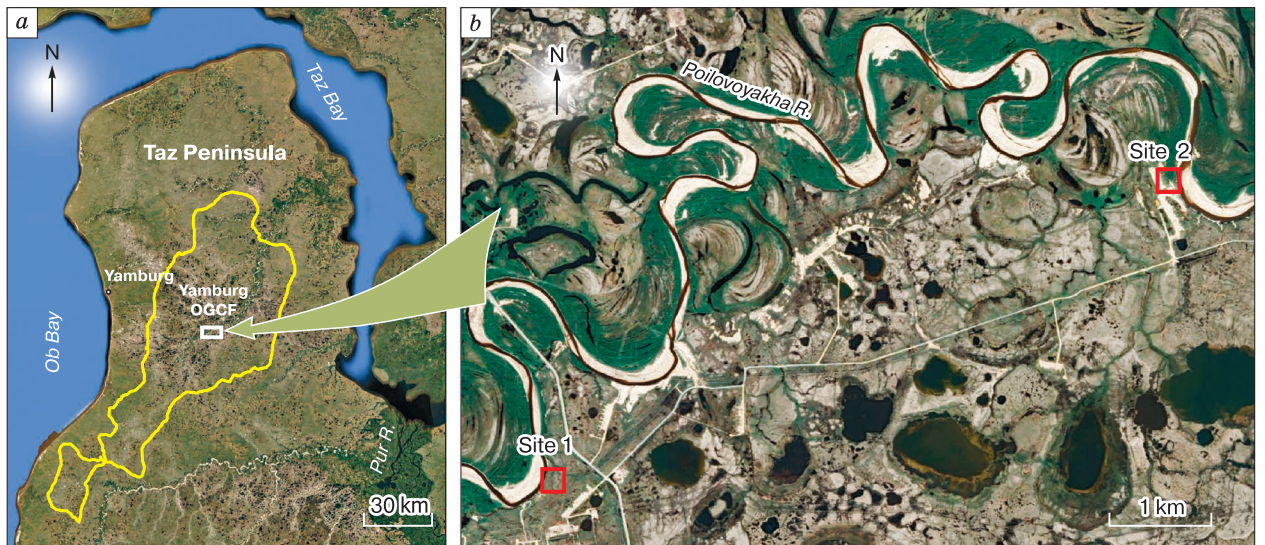


Fig. 1. Schematic maps of the (a) location of the Yamburg OGCF in the Taz Peninsula and (b) study sites 1 and 2.



**Fig. 2.** Sites of thermometric observations with (a) dwarf shrub-moss-lichen and (b) dwarf shrub-moss-herb vegetation covers in the area of the Yamburg OGCF.

bogging and wide distribution of lakes and flat-topped peatlands. Mosses, lichens, dwarf shrubs, and shrubs predominate in the vegetation cover.

The climate on the Taz Peninsula is maritime subarctic and is largely determined by its position close to the Kara Sea [Mel'nikov and Grechishchev, 2002]. The mean annual air temperature at the Yamburg OGCF is  $-7.8^{\circ}\text{C}$ , the mean annual precipitation is 350–390 mm, and the snow cover depth is 56–78 cm [Pavulin et al., 2015].

The study area belongs to the zone of continuous 300 to 400-m-deep permafrost. Permafrost temperatures at the zero-amplitude depth (7–10 m) range from  $-0.5$  to  $-3.5^{\circ}\text{C}$ . Permafrost includes epigenetically frozen sands and ice-bound loamy sands with a massive, rarely layered cryogenic texture. The active layer depth varies from 0.8 to 4.1 m and does not exceed 1.5 m in the areas with peat cover. The geological section of the study area to a depth of 10 m is represented by the Upper Pleistocene lagoon–marine sediments of the Zyryansky horizon. They are mostly overlain by the modern biogenic sediments–peat and by sediments of the technogenic origin (filled up soils) represented generally by fine sands [Pavulin et al., 2015].

Sites 1 and 2 near the Poilovoyakha River (red squares on Fig. 1b) were selected for thermometric measurements. The distance between the sites is about 6 km. Both sites are characterized by flat poorly dissected topography and are elevated at about 32 m a.s.l. The first two observation points (points 1 and 2) at site 1 characterize the area with drained peat on the surface dissected by an ice wedge of 20–

30 cm in width. This is the area of hummocky lichen-moss-dwarf shrub tundra (Fig. 2a).

At point 1 located right on the ice wedge, the ground cover is represented by a 12-cm-thick sphagnum moss (*Sphagnum fuscum*) mat with inclusions of haircap moss (*Polytrichum commune*) and lingonberry (*Vaccinium vitis-idaea*). At point 2, the ground cover consists of 12-cm-thick fruticose lichens (*Cladonia arbuscula*) underlain by peat.

Points 3 and 4 at Site 2 characterize the area with drained sandy soils and a relatively uniform dwarf shrub-moss-sedge (*Empetrum nigrum*, *Vaccinium vitis-idaea*, *Carex arctisibirica*) cover with some participation of low shrubs (*Ledum decumbens*, *Betula nana*) (Fig. 2b). The thickness of the vegetation cover at point 3 was 5 cm; at point 4, 2 cm. The depth of the active layer in this area ranged from 1.8 to 3.2 m. The distance between the observation points at each site did not exceed 1.5 m. To characterize weather conditions, we used data from the Yamburg weather station located 37 km west of the study area (Fig. 1a).

## METHODS

Temperature was measured by the autonomous loggers HOBO U23-003 with an accuracy of  $\pm 0.2^{\circ}\text{C}$ . Figure 3 demonstrates the installation scheme of the temperature sensors. At points 1 and 2, the bottom sensors were placed 12 cm below the surface, directly under the moss (without contact with ice) and lichen covers; at points 3 and 4, they were installed in the sandy soil, 12 cm below the surface of the vegetation cover.

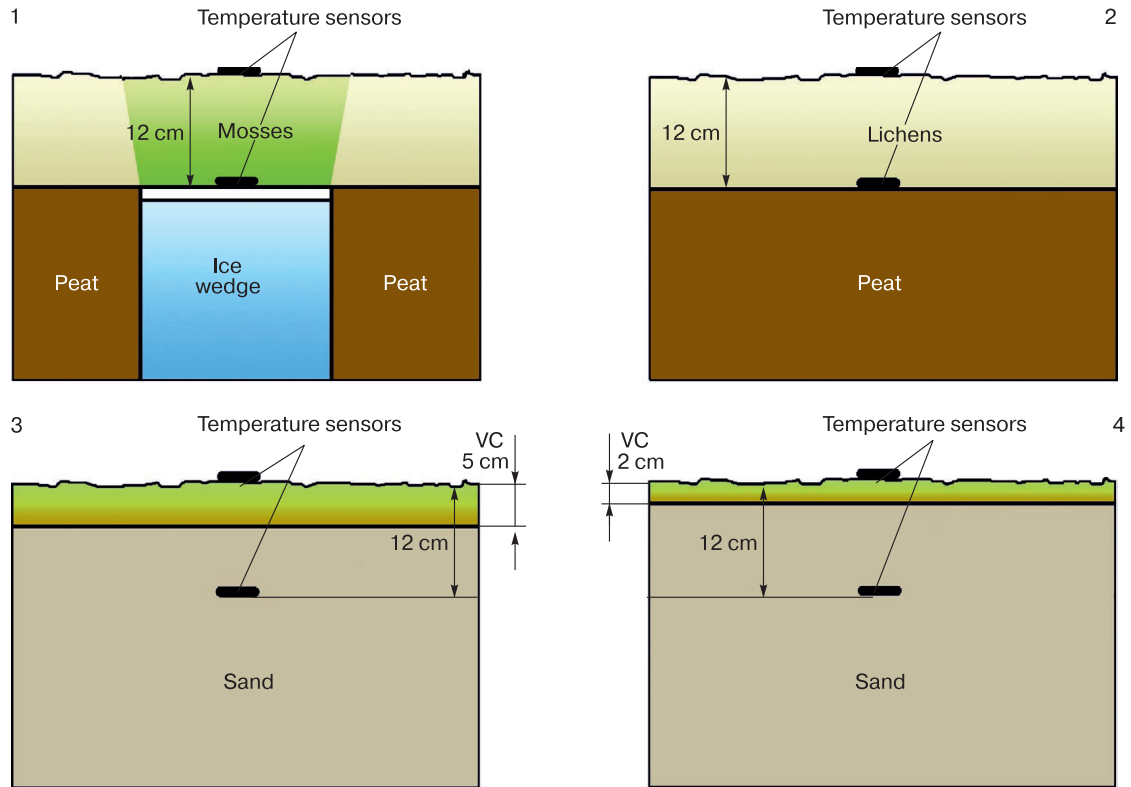


**Fig. 3. Schemes of the temperature sensor arrangement at observation points 1, 2, 3, and 4.**

VC – vegetation cover.

The sensors placed on the surface had shading canopies  $10 \times 30$  mm in size. As the distance between the observation points at each site did not exceed 1.5 m, the influence of the factors related to relief, insulation, and weather conditions was considered the same for both sites. Data were recorded after snowmelt from June 23 to August 26, 2013, at 30-min intervals. Data processing and analysis were performed using the HOBO Pro BHW and Excel Microsoft Office programs. Thermal diffusivity ( $K$ ), amplitude damping ( $M$ ) of the diurnal temperature fluctuation at a depth of 12 cm under the cover, and the thickness of the damping layer ( $D$ ) of DTF attenuation by 37 % were calculated by Eqs. (1)–(3). In practice, it is recommended to carry out measurements during 3–5 days under relatively stable weather conditions (without rain) and use them to determine the average value of parameter  $K$  [Ershov, 2004].

To characterize the relationship between parameters  $K$ ,  $M$ , and  $D$  and the specific features of weather conditions, the average values of these parameters were calculated for three evaluated periods of observations: A, B, C (Fig. 4, Table 2). These periods were characterized by relatively stable weather conditions, but differed in the mean air temperature ( $T_a$ ) and air humidity ( $W_a$ ).

In period A, anomalously high mean daily air temperatures were recorded; the temperatures at the surface of the ground cover reached  $40\text{--}50$  °C, and maximum daily temperature fluctuations at the surface were  $25\text{--}40$  °C. Period B was characterized by the air temperatures close to the mean values for the whole cycle of observations. During period C, relatively low air temperatures were recorded. Temperature records on the days of heavy rains were excluded from the analysis. Parameters  $K$ ,  $M$ , and  $D$  were calcu-

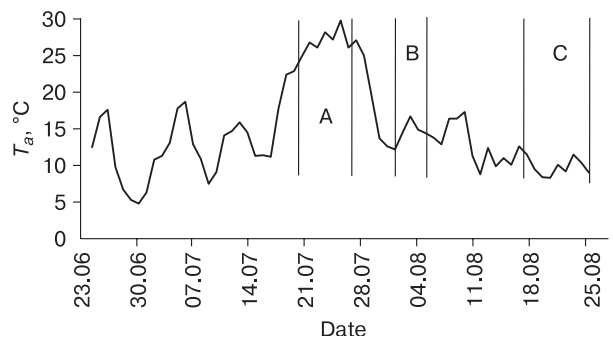


**Fig. 4. Mean daily air temperatures ( $T_a$ ) for the entire cycle of observations.**

A, B, and C are the periods of estimation of thermal diffusivity ( $K$ ) and parameters  $M$  and  $D$  for different weather conditions.

Table 2. Average values of thermal diffusivity ( $K$ ), parameter  $M$ , and damping depth ( $D$ ) of the cover samples for three periods of observations (A, B, C) with different values of air temperature ( $T_a$ ) and water content ( $W_a$ )

Point No.	Period A (June 21–27) $T_a = 27.3^\circ\text{C}$ ; $W_a = 49\%$			Period B (August 2–6) $T_a = 14.8^\circ\text{C}$ ; $W_a = 70\%$			Period C (August 18–26) $T_a = 9.8^\circ\text{C}$ ; $W_a = 79\%$		
	$K \cdot 10^7$ , $\text{m}^2/\text{s}$	$M$ , %	$D$ , cm	$K \cdot 10^7$ , $\text{m}^2/\text{s}$	$M$ , %	$D$ , cm	$K \cdot 10^7$ , $\text{m}^2/\text{s}$	$M$ , %	$D$ , cm
1	0.791	90.6	4.6	0.931	89.1	4.9	1.265	86.1	5.7
2	0.664	93.9	4.3	0.831	91.8	4.8	0.870	91.5	4.9
3	0.914	90.8	5.0	1.164	88.1	5.6	1.035	89.5	5.3
4	1.299	86.5	6.0	1.514	84.5	6.4	1.496	84.6	6.4

lated for each day after averaging the temperature data with a step of 2 h.

## RESULTS

In view of a relatively large distance (6 km) between the observation sites, the comparison of the results for the points located in close proximity to one another (1.5 m) can be considered more correct. Therefore, we compared the results separately for points 1 and 2 (Site 1) and 3 and 4 (Site 2). Figure 5

demonstrates the plots of the temperatures at the surface and under the SVC (data averaged for 3 days), mean squared deviation (MSD) of temperature distributions, mean values (horizontal lines), and difference ( $\Delta T$ ) of the mean temperatures at the surface and under the SVC during the entire period of observations. Position of the curves and MSD and  $\Delta T$  values indicate that, on average, during the summer, thermal insulation of the cover at point 1 was lower than at point 2 (Figs. 5a and 5b); at point 3, it was higher than at point 4 (Figs. 5c and 5d).

Figure 6 illustrates the plots of daily variations and mean values (horizontal lines) of  $K$  of the studied samples of SVC for the entire period of observations. During this period, thermal diffusivity  $K$  varied by an order of magnitude at point 1 (Fig. 6a) and by four times at point 2. At points 3 and 4, it varied by approximately three times (Fig. 6b). Such a significant variation of the actual values of thermal diffusivity was generally caused by the extreme variations in temperature, air humidity, and precipitation.

The mean values of  $K$ ,  $M$ , and  $D$  of the studied samples during three observation periods (A, B, C) are given in Table 2 and Figs. 7a, 7c, and 7d in the form of diagrams.

The difference in  $K$  for points 3 and 4 is quite natural, because the sand layer at point 4 is consider-

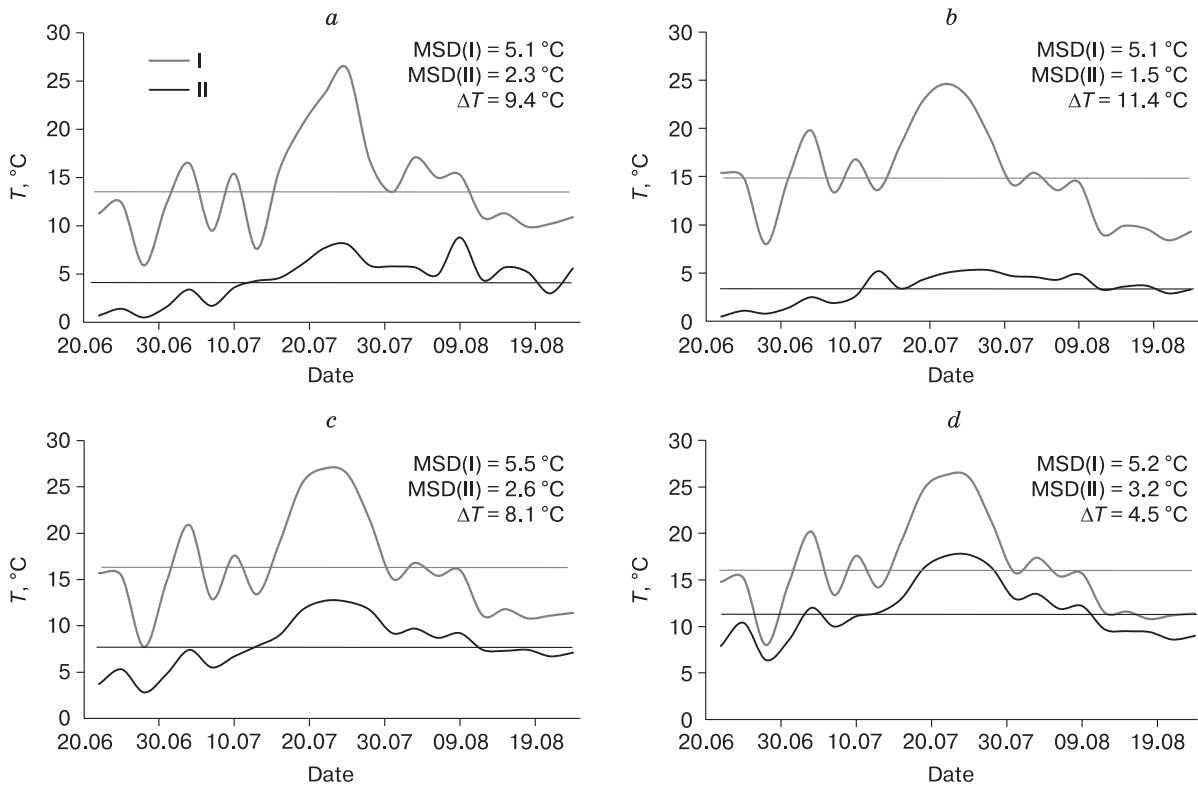


Fig. 5. Variations in temperatures ( $T$ ) averaged over 3 days at the surface (I) and under the soil-vegetation cover (II) at points 1–4 (a–d) over the entire period of observations.

MSD is the mean squared deviation of the temperature distribution;  $\Delta T$  is the difference between mean temperatures at the surface and under the soil-vegetation cover.

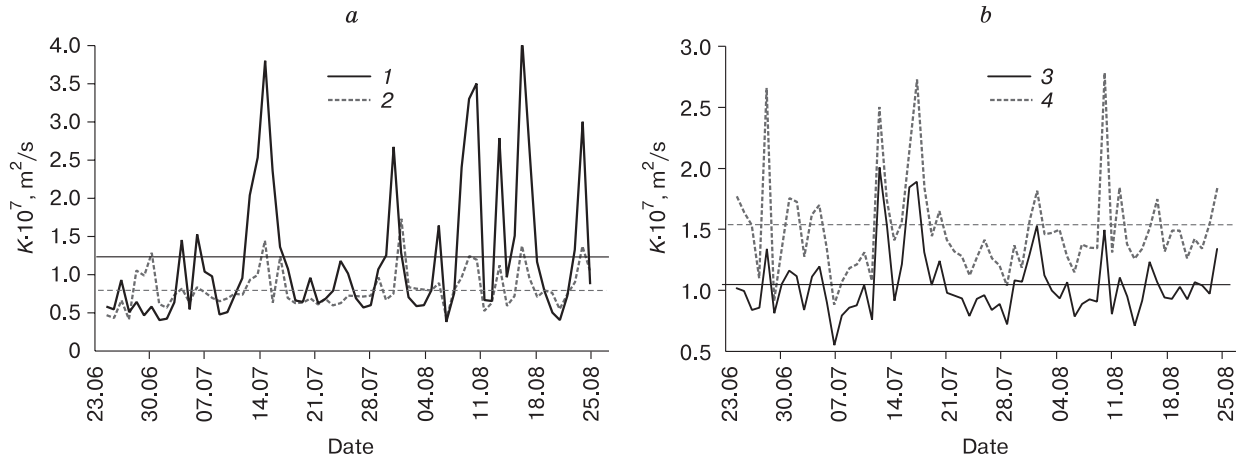


Fig. 6. Variations in thermal diffusivity ( $K$ ) over the entire period of observations at (a) Site 1 and (b) Site 2; 1–4 are the points of observations.

ably thicker than that at point 3. The values of  $K$  are significantly higher for sphagnum mosses than for lichens, especially during the “cold” period B. In comparison with other samples, moss is characterized by anomalously high MSD of thermal diffusivity values

for the estimated periods, especially, for the “cold” period B (Fig. 7b).

Average values of parameter  $M$ , which characterizes the degree of damping of daily temperature fluctuations at a depth of 12 cm, range from 84 to 94 %

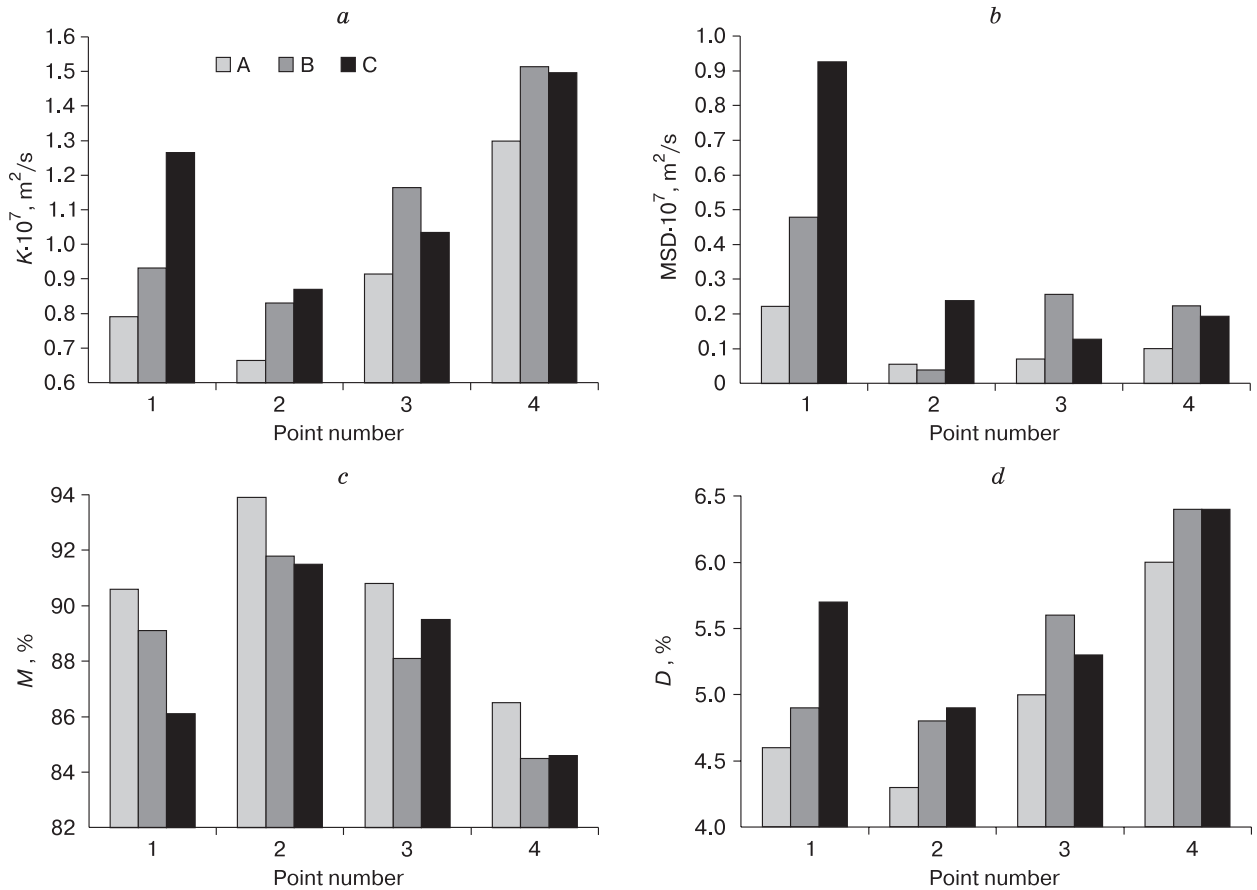


Fig. 7. Mean values (a) and mean squared deviation (MSD) (b) of thermal diffusivity ( $K$ ), parameter  $M$  (c), and damping depth ( $D$ ) (d) of the soil-vegetation samples by observation periods A, B, and C.

(Table 2, Fig. 7c). For the analyzed SVC types, the damping by 37 % (parameter  $D$ ) takes place in the near-surface layer with a thickness from 4.2 to 6.5 cm (Table 2, Fig. 7d).

## DISCUSSION

The average  $K$  values for points 1 (sphagnum) and 2 (lichen), obtained during the experiment (Table 2) are quite close to the published data on the analogous cover types (Table 1). This fact attests to the correctness of the measurements, calculations, and prospects for the use of temperature loggers to characterize thermal diffusivity for different types of the tundra SVC.

Thermal diffusivity values of sphagnum mosses and fruticose lichens do not differ significantly at the high and normal air temperatures (periods A and B) (Table 2, Fig. 7a). A decrease in air temperatures and, consequently, an increase in atmospheric moisture leads to an increase in  $K$  both for mosses and lichens. It is known that  $K$  of mosses and lichens is almost independent of temperature, but depends on the water content. Therefore,  $K$  may be mostly increased due to increasing the air humidity and intensity of precipitation by the end of summer. For lichens,  $K$  increased by a factor of 1.3 at most, which is close to  $K$  growth trends for some types of the tundra cover [Aleksyutina and Motenko, 2012; Porada et al., 2016] upon an increase in their water content. At the same time,  $K$  of mosses increased by 1.6 times during the transition from higher to lower air temperatures (Table 2, Fig. 7a). The difference in changes of thermal diffusivity under the same conditions for sphagnum and lichens may be related to the difference in the mechanisms of moisture saturation.

At points 3 and 4,  $K$  variations are almost the same and are less significant than those for sphagnum mosses (Table 2, Fig. 7a), which is indicative of identical and weak hygroscopic properties of the SVC at these points. Relatively high values of MSD of thermal diffusivity of sphagnum mosses for all periods of estimation (Fig. 7b) are most likely associated with their hygroscopic properties and heat exchange, because MSD of  $K$  for lichen sample is significantly lower.

Temperature measurements at the surface and at the bottom of the SVC indicate that, in summer, thermal insulating properties of sphagnum moss over the ice wedge are lower than those of fruticose lichens over peat (Figs. 5a and 5b). The average values of thermal diffusivity of sphagnum mosses calculated for each observation period were higher than those of lichens (Table 2, Fig. 7a). Similarly, for the SVC samples, including sandy soil and mixed vegetation with different thickness, the thermal insulating effect was higher in the sample with a lower  $K$  value (point 4). It follows that, under similar conditions, thermal diffu-

sivity for these types of the SVC can serve as an indicator of their thermal insulating properties in the same way as the thermal conductivity coefficient.

It was earlier shown that moisture saturation of live feather mosses (*Hylocomium splendens* and *Pleurozium schreberi*) reached only 40 % of the total water capacity, while live sphagnum (most often, *Sphagnum fuscum*) could be saturated up to 90 % of the total water capacity due to capillary rise of water [O'Donnell et al., 2009]. The thermal conductivity coefficients of live feather mosses and live sphagnum are almost equally dependent on the volumetric water content up to  $W_n = 40$  %. The only difference is that, in the real conditions, the water saturation of feather mosses and lichens is limited by the atmospheric moisture content, while sphagnum mosses can be additionally saturated by groundwater. By early autumn, the water content and thermal conductivity of all types of the SVC increase. However, the water content of sphagnum is significantly higher than that of feather mosses and fruticose lichens. During the transition to the frozen state,  $\lambda$  of feather mosses and lichens increases by 1.5–2 times. At the same time, owing to a higher water content,  $\lambda$  of sphagnum in the frozen state becomes several times higher than that of feather mosses and lichens. In this regard, sphagnum moss can be considered to have unique thermal insulating properties in drained areas thus preventing wedge ice from melting. During hot summer days, sphagnum moss is a good insulator, and during cold winter days, it is a good heat conductor [Park et al., 2018].

It was previously reported that the depth of the active layer under sphagnum mosses is significantly lower than that under green forest mosses and lichens [Bakalin and Vetrova, 2008; Fukui et al., 2008; Lorantya et al., 2018]. However, in the heavily watered areas, sphagnum significantly reduces its thermal insulating properties in summer, because it constantly occurs in the wet state and does not dry out even on hot days. In such areas, frozen soils under sphagnum occur deeper than in the areas with the normal water content of the soil cover [Kargopolov, 2001]. Therefore, when the sites are heavily watered and feather mosses and shrubby lichens are replaced by sphagnum mosses, an increase in the depth of the active layer is expected [O'Donnell et al., 2009].

## CONCLUSIONS

Variations in the effective values of thermal diffusivity of sphagnum mosses (*Sphagnum fuscum*, 12 cm thick) over the ice wedge and fruticose lichens (*Cladonia arbuscula*, 12 cm thick) over peat were characterized on the basis of continuous thermometric measurements in the area of the Yamburg oil and gas condensate field in the summer period. Additionally, measurements were performed for the two-layer

soil-vegetation samples (12 cm thick) consisting of the mixed vegetation cover (*Empetrum nigrum*, *Vaccinium vitis-idaea*, *Carex arctisibirica*) of 5 and 2 cm in thickness underlain by sandy soil. The obtained average values of thermal diffusivity for sphagnum mosses and fruticose lichens are quite close to the previously published values for these types of the tundra cover. This attests to the correctness of the measurements and calculations and to good prospects of using temperature loggers for *in situ* determination of thermal diffusivity of different types of the tundra soil-vegetation cover.

Compared to lichens, sphagnum mosses under the same weather conditions were characterized by a more significant *K* growth upon the decrease in the mean daily air temperature from 27.3 to 9.8 °C and the rise in relative air humidity from 49 to 79 %. This fact confirms the unique thermal insulating properties of sphagnum mosses for protecting wedge ice from melting, because sphagnum is a good insulator at high above-zero air temperatures and is a good heat conductor at subzero temperatures.

The results of temperature measurements pointed to a decrease in the amplitude of daily temperature fluctuations by 84–94 % at a depth of 12 cm under the studied soil-vegetation samples. A decrease by 37 % took place at a depth of 4.2–6.4 cm depending on the type of the vegetation cover. Variations in the damping depth of the amplitude of daily temperature fluctuations related to changes in the weather conditions were most significant for sphagnum mosses.

The results of this study confirm that, under real conditions, at the mean daily air temperature of 27 °C and below and the relative air humidity over 49 %, thermal diffusivity of the considered types of tundra soil-vegetation cover is indicative of its insulating properties.

**Acknowledgments.** *This study was conducted within the framework of state assignment No. AAAA-A19-119021590079-6 “Rational Nature Management and Efficient Development of Oil and Gas Resources in the Arctic and Subarctic Zones”.*

## References

- Aleksyutina, D.M., Motenko, R.G., 2012. Thermophysical properties of surface organic layers. In: Proc. 10<sup>th</sup> Intern. Conf. on Permafrost (Salekhard, June 25–29, 2012). Pechatnik, Tyumen, vol. 4, p. 13–14 (in Russian).
- Anisimov, O.A., Sherstyukov, A.B., 2016. Evaluating the effect of climatic and environmental factors on permafrost in Russia. *Earth's Cryosphere XX* (2), 78–86.
- Bakalin, V.A., Vetrova, V.P., 2008. Vegetation–permafrost relationships in the zone of sporadic permafrost distribution in the Kamchatka Peninsula. *Russ. J. Ecol.* **39** (5), 318–326.
- Beck, P.S.A., Goetz, S.J., 2011. Satellite observations of high northern latitude vegetation productivity changes between 1982 and 2008: ecological variability and regional differences. *Environ. Res. Lett.* **6**, 045501.
- Bhatt, U.S., Walker, D.A., Raynolds, M.K. et al., 2017. Changing seasonality of panarctic tundra vegetation in relationship to climatic variables. *Environ. Res. Lett.* **12**, 055003.
- Ershov, E.D. (Ed.), 2004. *Methods of Geocryological Research*. Izd. Mosk. Univ., Moscow, 512 p. (in Russian).
- Fel'dman, G.M., Tetel'baum, A.S., Shender, N.I., Gavril'ev, R.I., 1977. *Forecast of the Temperature Regime of Soils and the Development of Cryogenic Processes*. Nauka, Novosibirsk, 191 p. (in Russian).
- Fukui, K., Sone, T., Yamagata, K. et al., 2008. Relationships between permafrost distribution and surface organic layers near Esso, Central Kamchatka, Russian Far East. *Perm. Perigl. Proc.* **19**, 85–92.
- Gavril'ev, R.I., 2004. *Reference Guide on Thermophysical Properties of the Components of the Environment in the Permafrost Zone*. Nauka, Novosibirsk, 146 p. (in Russian).
- Gornall, J.L., Jonsdottir, I.S., Woodin, S.J., Van der Wal, R., 2007. Arctic mosses govern below-ground environment and ecosystem processes. *Oecologia* **153**, 931–941.
- Kargapolov, V.D., 2001. Influence of vegetation on the formation of perennially frozen rocks on the Okhotsk coast. *Kriosfera Zemli V* (4), 22–29 (in Russian).
- Konishchev, V.N., 2009. Permafrost response to climate warming. *Vestn. Mosk. Univ., Ser. 5: Geogr.*, No. 4, 10–20 (in Russian).
- Loranty, M.M., Berner, L.T., Taber, E.D. et al., 2018. Understorey vegetation mediates permafrost active layer dynamics and carbon dioxide fluxes in open-canopy larch forests of northeastern Siberia. *PLoS One* **13** (3), e0194014. – <https://doi.org/10.1371/journal.pone.0194014>
- Mandarov, A.A., Skryabin, P.N., 1978. Thermal conductivity of the soil of the Yenisei North and its seasonal dynamics. In: *Geothermophysical Research in Siberia*. Nauka, Novosibirsk, p. 74–82 (in Russian).
- Mel'nikov, E.S., Grechishchev, S.E. (Eds.), 2002. *Permafrost and Development of Oil and Gas Regions*. GEOS, Moscow, 402 p. (in Russian).
- Morozova, L.M., Magomedova, M.A., 2004. *Vegetation Cover Patterns and Plant Resources of the Yamal Peninsula*. Izd. Uralsk. Univ., Ekaterinburg, 63 p. (in Russian).
- O'Donnell, J.A., Romanovsky, V.E., Harden, J.W., McGuire, A.D., 2009. The effect of moisture content on the thermal conductivity of moss and organic soil horizons from black spruce ecosystems in interior Alaska. *Soil Sci.* **174** (12), 646–651.
- Osokin, N.I., Sosnovsky, A.V., 2012. Thermophysical properties of moss cover and its influence on the thermal regime of the ground, Spitsbergen Archipelago. In: Proc. 10<sup>th</sup> Intern. Conf. on Permafrost (Salekhard, June 25–29, 2012). Pechatnik, Tyumen, vol. 2, p. 313–316.
- Park, H., Launiainen, S., Konstantinov, P.Y. et al., 2018. Modeling the effect of moss cover on soil temperature and carbon fluxes at a tundra site in northeastern Siberia. *J. Geophys. Res.: Biogeosciences* **123** (9), 3028–3044.
- Pavlov, A.V., 1979. *Thermophysics of Landscapes*. Nauka, Novosibirsk, 284 p. (in Russian).
- Pavlov, A.V., 1980. *Calculation and Regulation of the Permafrost Soil Regime*. Nauka, Novosibirsk, 240 p. (in Russian).
- Pavlinin, V.B., Bykova, A.V., Lobastova, S.A., 2015. Monitoring of technogenic gully formation at hydrocarbon production facilities in permafrost conditions. *Inzhenern. Izysk.* **3**, 60–68 (in Russian).

- Porada, P., Ekici, A., Beer, C., 2016. Effects of bryophyte and lichen cover on permafrost soil temperature at large scale. *The Cryosphere* **10**, 2291–2315.
- Soudzilovskaia, N.A., Van Bodegom, P.M., Cornelissen, J.H.C., 2013. Dominant bryophyte control over high-latitude soil temperature fluctuations predicted by heat transfer traits, field moisture regime and laws of thermal insulation. *Function. Ecol.* **27**, 1442–1454.
- Stepanenko, V.M., Repina, I.A., Fedosov, V.E. et al., 2020. An overview of parameterizations of heat transfer over moss-covered surfaces in the Earth system models. *Izv., Atmos. Ocean. Phys.* **56** (2), 101–111.
- Stoy, P.C., Street, L.E., Johnson, A.V. et al., 2012. Temperature, heat flux, and reflectance of common subarctic mosses and lichens under field conditions: might changes to community composition impact climate-relevant surface fluxes? *Arct. Antarc. Alp. Res.* **44** (4), 500–508.
- Urban, M., Forkel, M., Eberle, J. et al., 2014. Pan-Arctic climate and land cover trends derived from multi-variate and multi-scale analyses (1981–2012). *Rem. Sensing* **6**, 2296–2316.
- URL: <https://earth.google.com.my/> (last visited: September 17, 2021).
- Vasil'ev, A.A., Gravis, A.G., Gubar'kov, A.A. et al., 2020. Permafrost degradation: results of the long-term geocryological monitoring in the western sector of Russian Arctic. *Earth's Cryosphere XXIV* (2), 14–26.

*Received April 13, 2021*  
*Revised December 30, 2021*  
*Accepted January 3, 2022*

*Translated by V.A. Krutikova*